# Anomalous Diffusion of Probe Molecules in Polystyrene: Evidence for Spatially Heterogeneous Segmental Dynamics

**Marcus T. Cicerone, F. R. Blackburn, and M. D. Ediger***

*Department of Chemistry, University of Wisconsin—Madison, Madison, Wisconsin 53706*

*Received July 18, 1995; Revised Manuscript Received September 14, 1995*[⊗]

ABSTRACT: A holographic fluorescence recovery after photobleaching technique has been used to measure the translational motion of tetracene and rubrene (tetraphenyltetracene) in polystyrene (PS) from $T_g$ − 10 K to $T_g$ + 100 K ($T_g$ = 373 K). At 363.5 K, the translational motion of tetracene is not diffusive; i.e., the mean-square displacement is not linear in time on the length scale (60 nm) and time scale (10 h) of the experiment. Above 370 K, diffusive transport is observed for both probes with diffusion coefficients in the range of $10^{-6}$–$10^{-15.5}$ cm²/s. The observed diffusion coefficients have a significantly weaker temperature dependence than rotation times for these two probes in PS. At low temperatures, the root-mean-square displacement for tetracene approaches 60 nm in one rotational correlation time. It is not necessary to conclude, however, that individual probe molecules translate large distances without rotating. All these observations can be rationalized without invoking a change in the local relationship between rotation and translation if the local dynamics of PS are assumed to be spatially heterogeneous.

## I. Introduction

The diffusion of small molecules in polymers has been actively studied for several decades.[1] Small molecule diffusion is integrally related to drug delivery rates and polymer dissolution.[2] The plasticization, coloration, curing, and drying of coatings (e.g., paint) are all influenced by the mobility of solvents, dyes, and various low molecular weight additives.[3] Diffusion studies provide considerable insight into the fundamental molecular motions of an amorphous polymer matrix.[1,4–12] The diffusion of small molecules can also provide information about polymer morphology and rates of polymerization.

If we define the diffusion coefficient in terms of the mean-square displacement as follows,

$$D_T = \lim_{t\to\infty} \frac{\langle r^2 \rangle}{6t} \tag{1}$$

we can ask how $D_T$ for a probe molecule is influenced by the dynamics of an amorphous polymer host. $D_T$ values for gas molecules in amorphous polymers are known to have a much weaker temperature dependence than that of the viscosity $\eta(T)$.[13,14] The picture of gas transport emerging from recent computer simulations is one of hops of ~10 Å between cavities in the matrix.[15] These hops are facilitated by high-frequency vibrational motions (>$10^{11}$ Hz) with a weak temperature dependence.

In contrast to gaseous probe molecules, the translational motion of solvent molecules and larger probes is coupled significantly with the conformational dynamics of the polymer host. In low-$T_g$ amorphous polymers, Ferry and co-workers found that the diffusion of flexible and rigid probes with molecular weights on the order of 200 has the same temperature dependence as $\eta$.[7,8] In a study of five higher $T_g$ polymers, Ehlich and Sillescu found that probes of about the same size had diffusion coefficients with a somewhat weaker temperature dependence than $\eta$ ($D_T \propto \eta^{-\xi}$ with $0.50 < \xi < 0.84$).[4] Other experiments on probe diffusion in high-$T_g$ polymers are broadly consistent with the work of ref 4.[9,12,16]

Typically, probe diffusion studies in bulk amorphous polymers are interpreted in terms of free volume theory.[1,17] Using this approach, one interprets the temperature dependences of $D_T$ and $\eta$ in terms of coupling between probe and matrix motion. If the temperature dependence of $D_T$ for a rigid probe is weaker than that of $\eta$, one concludes that the probe is too small to be fully coupled with the segmental motions of the polymer. This interpretation may need to be reevaluated in some cases, however, given recent results concerning the relationship between translational and rotational diffusion in small molecule glass formers[18–20] and polymers.[21] In a number of cases, translational diffusion has a significantly weaker temperature dependence than $\eta$ *while rotational motion has a temperature dependence which does not differ significantly from that of* $\eta$. A straightforward application of the free volume approach would lead to the odd conclusion that translational motion is partially decoupled from matrix motions while rotational motion is fully coupled.

In this paper, we present translational diffusion measurements of tetracene and rubrene in polystyrene (PS) from $T_g$ − 10 K to $T_g$ + 100 K ($T_g$ = 373 K). A holographic fluorescence recovery after photobleaching (holographic FRAP) technique was used to measure $D_T$ from $10^{-6}$ to $10^{-15.5}$ cm²/s. A unique feature of these measurements is that the rotational correlation times for these probes in PS have been recently reported.[22] Thus, for the first time in a polymer system, the rotation and translation of the same probe can be compared as a function of temperature. We find that $D_T$ has a significantly weaker temperature dependence than $\eta$ while the rotational correlation times scale with $\eta$. For tetracene, these two temperature dependencies are so different that at 363 K we observe translational motion across 50 nm (40 probe lengths) in one rotational correlation time!

We observe translational motion which is not diffusive for tetracene in PS at 363 K. Thus, the time and length scales of our measurement are sufficiently small that $\langle r^2 \rangle/t$ has not reached its asymptotic limit (see eq 1). To our knowledge, this is the first report of such anomalous probe diffusion across tens of nanometers in a bulk amorphous polymer.

[⊗] Abstract published in *Advance ACS Abstracts,* November 1, 1995.

0024-9297/95/2228-8224$09.00/0 

We can qualitatively account for these observations if the local dynamics of PS are spatially heterogeneous and if the heterogeneity becomes more prominent as the temperature is lowered toward $T_g$. This explanation assumes that both rotational and translational probe motion are completely coupled with the matrix motions responsible for the glass transition. The different temperature dependences of probe rotation and translation are due to the different ways in which rotation and translation experiments average over spatially heterogeneous dynamics. The observation of anomalous translational diffusion of tetracene near $T_g$ provides some indication of the length scale of the heterogeneity.

## II. Experimental Section

**Samples.** Polystyrene (PS) was obtained from Polysciences ($M_w$ = 50 000, $M_w/M_n$ = 1.06). Rubrene and tetracene were obtained from Aldrich. Samples of rubrene or tetracene in PS were prepared by freeze-drying. A dilute solution of PS and probe in benzene was sprayed into a round-bottom flask at 77 K. The benzene sublimed under vacuum while the temperature of the flask was slowly increased, always keeping $T < T_g$ of the remaining PS/benzene mixture. Finally, the sample was brought to 360 K for ~1 h. $T_g$ values of the probe/PS samples were checked by DSC and found to agree with the $T_g$ of the PS as supplied ($T_g$ = 373 K at 10 K/min, using midpoint convention), confirming that all benzene had been removed. The probe concentration (<25 ppm) was low enough that the sample was not plasticized and that the results reported are expected to be independent of probe concentration.

Free-standing samples were used for experiments below 395 K. To prepare these samples, the probe/PS mixture was formed into a disk (1 mm thick) using a KBr press. These disks were annealed to remove birefringence. For experiments at $T \geq 395$ K, the freeze-dried samples were placed in a 2 mm × 6 mm cuvette and heated to 473 K under vacuum until an optically clear sample was obtained. Either the disks or the cuvettes were placed in a 1 cm$^2$ cuvette which was filled with silicone oil. The silicone oil acted as both an index matching fluid and a temperature bath. The silicone oil did not plasticize the PS disks.[23] Sample temperatures were constant to within ±0.05 K during any given experiment. The reported temperatures are correct to within 0.2 K absolute accuracy.

All the data presented here (even for temperatures lower than the DSC $T_g$) represent dynamics in the *equilibrium* polymer melt. Effects of thermal history were eliminated by holding samples at constant temperature and repeating measurements until the results no longer depended upon ageing time. At 363.5 K, samples were aged 3−5 days.

**Holographic FRAP Technique.** The holographic fluorescence recovery after photobleaching (FRAP) technique was first used by Davoust et al.[24] Some details of the method are provided here so that we can clearly describe two modifications which we have made in order to measure very small diffusion coefficients. The basic method is illustrated in Figure 1. Two intense writing beams are crossed in the sample to produce an interference pattern. Photobleachable probes are selectively destroyed in regions of constructive interference; these regions are darkened at the top of the figure. After substantial attenuation, the same two beams are used to "read" the periodic pattern of probe concentration. The phase of one beam is modulated relative to the other so that the reading grating is swept across the written grating at a constant velocity. Each time the reading grating is out of phase with the written grating, a maximum will be observed in the probe fluorescence signal; at these times, the bright regions of the reading grating overlap with regions of the sample where little bleaching has occurred, as shown in the figure. The modulation of the fluorescence signal eventually decays due to translational motion of the unbleached probes. A schematic diagram of the experimental apparatus is shown in Figure 2.

**Writing the Grating.** The holographic intensity grating created when two coherent beams are crossed in a sample can

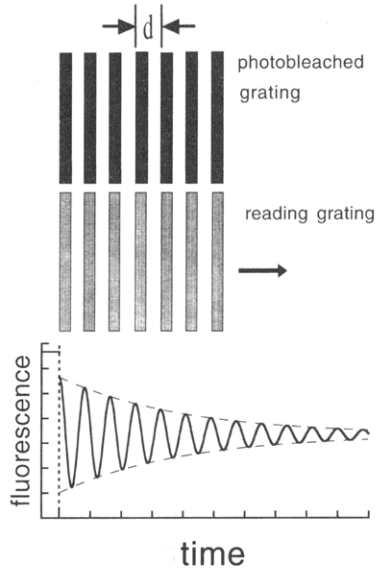


**Figure 1.** Pictoral explanation of the holographic FRAP experiment.

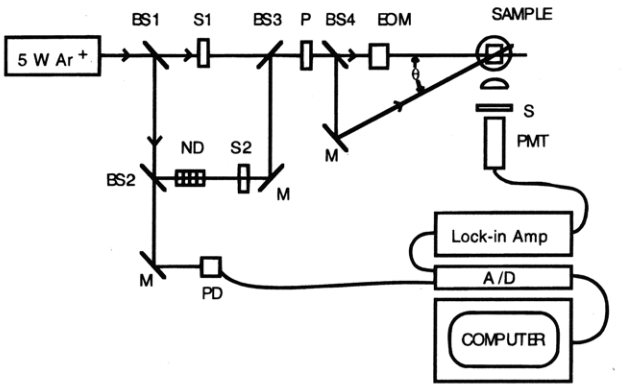


**Figure 2.** Schematic of holographic FRAP apparatus: BS, beam splitter; P, polarizer; S, shutter; M, mirror; ND, neutral density filter; PD, photodiode; A/D, analog to digital converter; EOM, electrooptic modulator; PMT, photomultiplier tube. The writing and reading beams are controlled by shutters S1 and S2, respectively. Shutter S protects the PMT during writing.

be described by[25,26]

$$I(x,\phi) = \frac{1}{2} + \frac{1}{2}\cos(qx + \phi) \tag{2}$$

Here $\phi$ is the phase difference between the two beams. The grating wavevector $q$ and the grating period $d$ are determined by the angle $\theta$ at which the beams are crossed:

$$d = \frac{2\pi}{q} = \frac{\lambda}{2\sin(\theta/2)} \tag{3}$$

Equation 3 applies to copropagating beams; for counterpropagating beams ($\theta = 180°$), $\lambda$ in the numerator must be replaced by $\lambda/n$.[27]

A periodic concentration profile of unbleached probe molecules $C(x,t)$ is created upon bleaching with crossed beams. $C(x,t)$ can be described as

$$C(x,t) = \sum_{n=0}^{\infty} B_n(t)\cos(nqx) \tag{4}$$

where $B_n(t)$ are time-dependent spatial Fourier components. Although, as eq 2 indicates, the light intensity grating only contains Fourier components at $k = 0$ and $k = q$, $C(x,t)$ can contain higher-order components because of saturation or nonlinearities in the photobleaching reaction.

Typical bleaching times in these experiments ranged from 1 ms to 3 s using 0.1−0.5 W at 488 nm; typical spot sizes ranged from 0.5 to 3 mm. Grating periods ranged from 0.15 to 370 $\mu$m. The $Ar^+$ laser was operated in single-frequency mode. For rubrene and tetracene, photobleaching is believed to occur through an excited state reaction with $O_2$.[28]

**Reading the Grating.** Since the reading beams are collinear with the writing beams, they produce a grating with the same period. The reading beams are attenuated by roughly $10^6$ relative to the writing beams so that very little residual photobleaching occurs during reading. We monitor the time dependence of $C(x,t)$ via the intensity of fluorescence induced by the reading grating as the phase of one reading beam is modulated. The fluorescence signal is given by

$$F(t,\phi) = \int_{-l/2}^{l/2} I(x,\phi)C(x,t)\,dx \tag{5}$$

Here $l$ is the length of the grating in the sample. In the limit that $l \gg 1/q$, the only Fourier components of $C(x,t)$ which are detected are $B_0$ and $B_1$:

$$F(t,\phi) \approx \int_{-l/2}^{l/2} I(x,\phi)[B_0(t) + B_1(t)\cos(qx)]\,dx \tag{6}$$

Modulation of $\phi$ produces a modulation in $F(t,\phi)$, allowing the separation of $B_0(t)$ and $B_1(t)$.

Vibrations can have a significant influence on the holographic FRAP experiment because they can produce random fluctuations in $\phi$. For example, in the counterpropagating geometry, sample motion of only 75 nm produces a phase shift of $\pi$ if the optics that guide the reading beams do not move with the sample. Use of an air-cushioned laser table effectively damped high-frequency (>10 Hz) vibrations. The existence of lower frequency vibrations dictated our choice of a modulation scheme. The phase of one reading beam is repeatedly ramped from 0 through $2\pi$ at 10 kHz using an electrooptic modulator (Conoptics). Because the transition in phase from $2\pi$ back to 0 is very fast (<1 $\mu$s), the reading grating effectively translates at a constant velocity with respect to $C(x,t)$. This modulation scheme concentrates the signal due to $B_1(t)$ in a narrow frequency band regardless of any slow phase changes caused by vibrations. This is not the case for the sinusoidal modulation previously used with the holographic FRAP experiment.[24,29,30] In the present study, a two-phase lock-in amplifier (Stanford Research) was used to determine the modulation amplitude ($=2B_1(t)$). $B_0(t)$ is simply the average of $F(t,\phi)$ over many modulation cycles.

We define the contrast of the grating written in the sample as:

$$c(q,t) = B_1(t)/B_0(t) \tag{7}$$

Although we are primarily interested in $B_1(t)$, division by $B_0(t)$ compensates for any changes in $B_1(t)$ due to residual bleaching of the probe molecules by the reading beams.

**Translational Motion.** Since changes in $C(x,t)$ are monitored through fluorescence, and since only the unbleached probe molecules absorb the laser light and fluoresce, the holographic FRAP experiment measures the translation of only the unbleached probe molecules.[31] The function obtained directly from the experiment, $c(q,t)$, is proportional to the spatial Fourier transform of the single-particle van Hove function:

$$c(q,t)/c(q,0) = \int_{-\infty}^{\infty} G_s(x,t)e^{iqx}\,dx \equiv c(t) \tag{8}$$

When translational motion is diffusive, $G_s(x,t)$ is Gaussian and the translational relaxation function $c(t)$ decays exponentially:

$$c(t) = e^{-t/\tau_T} \tag{9}$$

The relationship between the translational relaxation time $\tau_T$ and the diffusion coefficient $D_T$ is given by

$$D_T = \frac{1}{q^2\tau_T} = \frac{d^2}{4\pi^2\tau_T} \tag{10}$$

In the case that translational motion is not diffusive, $c(t)$ will not decay exponentially, and we can define a characteristic decay time for the translational relaxation function as

$$\tau_T \equiv \int_0^{\infty} c(t)\,dt \tag{11}$$

In order to facilitate the integration of eq 11, we approximate $c(t)$ as a Kohlrausch−Williams−Watts (KWW) decay plus an exponential as follows:

$$c(t) \approx ae^{-(t/\tau_1)^\beta} + (1-a)e^{-t/\tau_2} \tag{12}$$

This function fits the data adequately and is used for no other reason. Although eq 10 is not strictly valid when the decay of $c(t)$ is nonexponential, we use it in this regime for the purpose of comparison to other data.

**Elimination of Rotation Artifacts.** The description of the holographic FRAP experiment presented above ignores the potential influence of molecular rotation on the fluorescence induced by the reading beams. If the probe rotation time $\tau_c$ is much less than the bleaching time, the above description is correct. If $\tau_c$ is longer than the bleaching time but less than $\tau_T/100$, some of the contrast created by bleaching will decay via rotation, but the shape of $c(t)$ will not be affected. Hence the correct $D_T$ will be calculated. If $\tau_c$ is comparable to $\tau_T$, rotational relaxation can distort the observed decay of $c(t)$.

The effects of rotation can be removed from the fluorescence signal by observing fluorescence at an angle that is insensitive to probe rotation. From the work of Wegener et al.,[32] it can be shown that if a 90° fluorescence detection geometry is used, the writing and reading beams should be polarized at +45° and −19.7° from vertical, respectively, and an analyzer polarizer should be set at 35.2° from vertical. This completely eliminates any influence of rotation on $c(t)$. We have used this scheme whenever rotation could effect the shape of $c(t)$ ($\tau_c \geq \tau_T/100$). In all other cases, we have not used this scheme since higher signal levels are available when reading and writing beams are all vertically polarized and no analyzer is used.

**Comparison of Holographic FRAP to Other Techniques.** The holographic FRAP technique is quite similar to other FRAP methods.[33-35] The major advantage of the holographic approach is that $d$ spacings as small as $\lambda/2n$ can be achieved (using the counterpropagating geometry). In addition, since the reading grating in the holographic method contains only a single wavevector, the signal is exactly the Fourier transform of $G_s(x,t)$ (eq 8). Typically, the reading patterns used in other FRAP experiments contain higher Fourier components.

Forced Rayleigh scattering (FRS) has two advantages relative to the holographic FRAP technique. Many of the probes typically used in FRS have higher quantum yields for photoactivation than do rubrene and tetracene. Thus less laser power is required to write the grating. If the FRS probe does not absorb light of the wavelength of the reading beam, the reading beam will not perturb the written grating. In constrast, a very low reading beam intensity is required in the holographic FRAP experiment to minimize residual bleaching.

The major disadvantage of FRS relative to the holographic FRAP experiment is that generally the diffusion of both the dye and its photoproduct contributes to grating decay. This limits the accuracy with which diffusion coefficients can be determined[36] and means that information about the shape of $G_s(x,t)$ is not easily obtained from the observed decay. In addition, the holographic FRAP experiment is easier to line up and is not influenced by static inhomogeneities in the index of refraction of cells, samples, and optics. It is also easier to

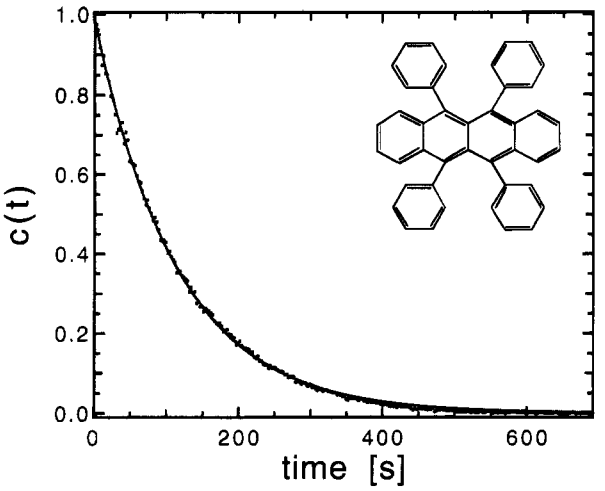


**Figure 3.** Translational relaxation function $c(t)$ for rubrene in PS (T = 386 K, $d$ = 0.153 $\mu$m). The solid line is a single-exponential fit to the data with $\tau_T$ = 116 s. The structure of rubrene is also shown.

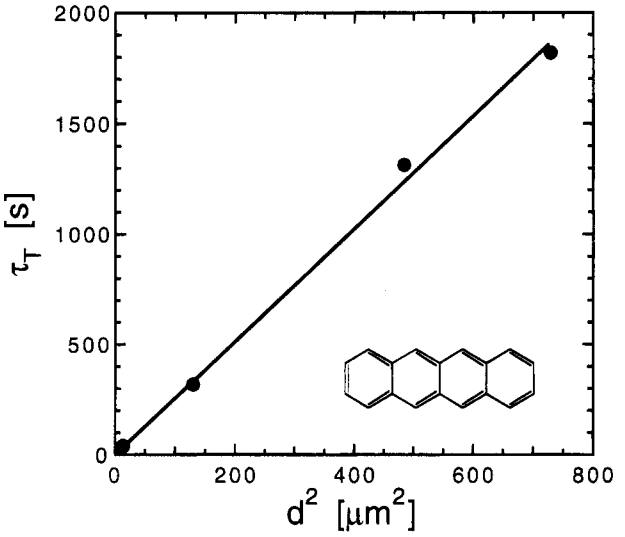


**Figure 4.** Translational relaxation times at four different grating spacings for tetracene in PS at 396.8 K. The solid line is a linear least-squares fit to the data with intercept at zero and a slope of $(4\pi^2 D_T)^{-1}$, where $D_T = 1.0 \times 10^{-10}$ cm$^2$ s$^{-1}$. The structure of tetracene is also shown. Errors in $\tau_T$ and $d$ are 10 and 2%, respectively.

use at small angles where it can be difficult to separate the diffracted and transmitted beams in an FRS experiment.

## III. Results

Figure 3 shows a typical translational relaxation function $c(t)$ obtained with the holographic FRAP technique. The sample was rubrene in PS at 386 K. Counterpropagating writing beams were used to produce the smallest possible grating period that can be obtained on this sample ($d$ = 0.153 $\mu$m). As shown by the fit in the figure, the data are well described by a single exponential. Since the observed signal is the spatial Fourier transform of $G_s(x,t)$ (see eq 8), the observed exponential decay indicates that $G_s(x,t)$ is Gaussian. Hence, the observed translational motion of rubrene molecules in PS is diffusive at this temperature.

The dependence of the translational relaxation time $\tau_T$ on the grating period provides another method for establishing whether translational motion is diffusive. Figure 4 displays $\tau_T$ as a function of $d^2$ for tetracene in PS at 397 K. In agreement with eq 10, a linear

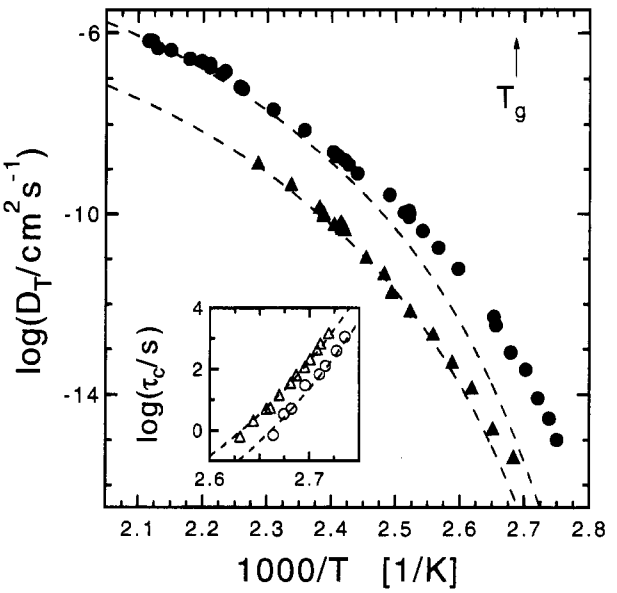


**Figure 5.** Translational diffusion coefficients (main figure) and rotational correlation times (inset) as a function of inverse temperature in PS. Translation: (▲) rubrene; (●) tetracene. Rotation: (△) rubrene; (○) tetracene. The dashed lines show the temperature dependence of $T/\eta$ (main figure) and $\eta/T$ (inset). Translational diffusion has a significantly weaker temperature dependence than rotation. The rotation data have been published previously.[22]

dependence is observed with an intercept of zero. Thus, the observed translation is diffusive; the diffusion coefficient can be obtained from the slope. Qualitatively, Figure 4 indicates that the mean-square displacement is linear in time as expected for diffusive motion.

Translational diffusion coefficients for rubrene and tetracene in PS are shown as a function of inverse temperature in Figure 5. With the exception of the lowest temperature points for tetracene, the grating decays for both probes were always well fit by a single exponential. As discussed below, a nonexponential decay was observed for tetracene at 363 K; for this point, $D_T$ was estimated using eqs 10–12.

The dashed lines in Figure 5 show the temperature dependence of $T/\eta$ for PS.[37] The comparison between $D_T$ and $T/\eta$ is partially motivated by the Stokes–Einstein equation, which predicts the translational diffusion coefficient for a sphere in a hydrodynamic continuum:

$$D_T = kT/6\pi\eta r_s \qquad (13)$$

Here, $k$ is Boltzmann's constant and $r_s$ is the radius of the sphere. While our probes are not spheres and PS is not a hydrodynamic continuum, one might expect the diffusion of a sufficiently large probe to have the temperature dependence of $T/\eta$. Clearly $D_T$ values for tetracene and rubrene have a weaker temperature dependence than $T/\eta$.

A second reason for the comparison of temperature dependencies shown in Figure 5 is related to the inset in this figure. Here rotational correlation times $\tau_c$ are shown for rubrene and tetracene near $T_g$ in PS.[22] The rotation data follow the temperature dependence of $\eta/T$ in the same temperature range where $D_T$ has a significantly weaker temperature dependence.

Figure 6 shows a direct comparison between $\tau_T$ (for $d$ = 0.153 $\mu$m) and $\tau_c$ for tetracene in PS. The points for $T$ > 380 K were obtained by scaling $\tau_T$ values obtained

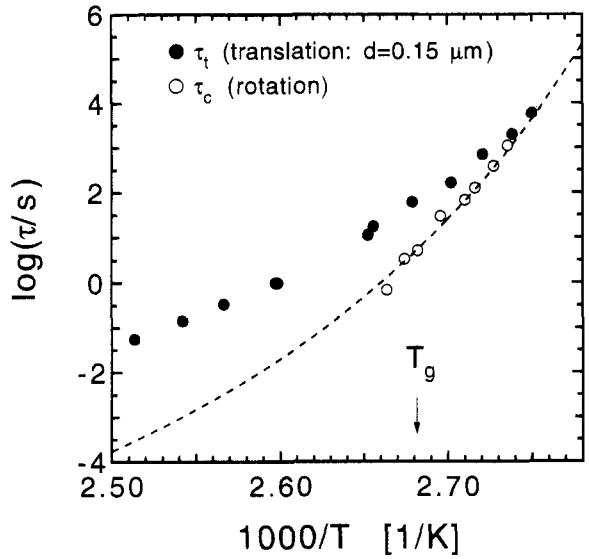


**Figure 6.** Comparison of relaxation times for tetracene in PS: (●) translational relaxation time with $d$ = 153 nm; (○) rotational correlation time. At low temperature, the average time needed to translate 60 nm is comparable to the rotational correlation time.

at $d$'s larger than those expected for $d$ = 0.153 μm according to eq 10. Remarkably, at the lowest temperatures, the time required for tetracene to translate a substantial fraction of 0.153 μm is comparable to the average probe rotation time. We will return to this comparison in section IV. Both the rotation and translation data were obtained from equilibrium samples which had been allowed to age until the results were independent of sample aging time. Thus these results are not artifacts associated with quenched or poorly aged samples.

**Anomalous Diffusion.** Figure 7 displays $c(t)$ for tetracene/PS at 370.0 (a) and 363.5 K (b). Both data sets were obtained with counterpropagating writing beams ($d$ = 0.153 μm). The observed decay at 370 K is exponential to a good approximation, as indicated by the straight line fit in the inset. The decay at 363.5 K is clearly nonexponential and appears to exhibit two distinct time scales for relaxation. The faster relaxation can be described by a KWW decay with $\beta$ = 0.8 (see eq 12). The slower relaxation accounts for ~20% of the decay and is nearly exponential; it has a characteristic relaxation time of roughly 10 times that of the faster relaxation.

The nonexponential decay in Figure 7b indicates that $G_s(x,t)$ under these conditions is not Gaussian (see eq 8). Thus, the translational motion of tetracene molecules in PS at 363.5 K is not diffusive on the length and time scales of our experiment. To our knowledge, this is the first observation of such anomalous diffusion of probes in bulk polymers. This behavior is most naturally explained by spatially heterogeneous dynamics, as we discuss in the next section.

It would be very difficult to test the dependence of $\tau_T$ on $d^2$ for the conditions shown in Figure 7b because of the very large values of $\tau_T$ expected at larger $d$'s. The acquisition time for one data set with $d$ = 0.153 μm at 363.5 K was ~10 h. The next larger grating spacing available with our apparatus is ~10 times larger; thus a ~40 day decay time would be expected.

We emphasize that the nonexponential decay shown in Figure 7b is not an artifact of the experimental geometry since counterpropagating writing beams were

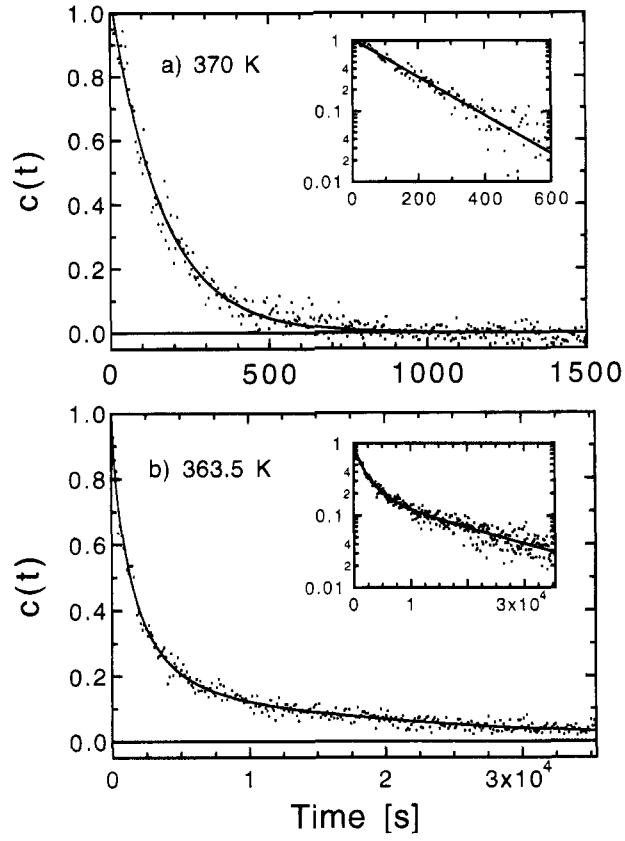


**Figure 7.** Time dependence of the translational relaxation function ($d$ = 153 nm) for tetracene/PS at two temperatures: (a) 370 K. The solid line is a single-exponential fit to data. (b) 363 K. The solid line is a fit to the data using eq 12.

used to collect both data sets shown in Figure 7. We also considered the possibility that the nonexponential decay might be due to the influence of probe rotation. In section II, we describe how changes in the fluorescence signal associated with probe rotation can be completely suppressed. This method was used to acquire the data in both parts of Figure 7. The exponential decay observed in Figure 7a verifies that this method works, since at this temperature probe rotation occurs on a time scale of roughly $\tau_T$/5 and does influence the shape of the observed decay if the method is not used. Finally, we reiterate that both samples in Figure 7 were aged until the observed decays no longer depended upon aging time.

## IV. Discussion

**Translation vs Rotation.** We return to Figures 5 and 6 in order to emphasize the unusual nature of these results. Figure 6 shows that the translational relaxation time for tetracene in PS at 363.5 K (1000/$T$ = 2.75) is approximately equal to the rotational correlation time $\tau_c$ expected at this temperature (based on a small extrapolation). How far has the average tetracene molecule translated in this time? Although translation is not strictly diffusive under these conditions, we can approximately calculate the mean square displacement as $\langle r^2 \rangle \approx 6D_T\tau_c \approx 3d^2/(2\pi^2) = (60\ \text{nm})^2$. Tetracene is ~1.3 nm in length with an average radius of ~0.5 nm. *Thus, on the average, tetracene molecules translate ~50 times their length in the average time required for a tetracene to rotate!* This statement does not imply that any individual tetracene molecule translates large distances without rotating (see below).

Similar calculations may be done for other temperatures. At 370 K, the root-mean-square (rms) displace-

ment for tetracene in a time $\tau_c$ is 26 nm. This indicates that strongly enhanced translational motion is observed even at temperatures where diffusive transport is observed in the holographic FRAP experiment. The rms displacement for tetracene in a time $\tau_c$ at 450 K is 3 nm, 20 times smaller than the result at 363 K. This last calculation assumes that $\tau_c$ is proportional to $\eta/T$ at higher temperatures than those shown in the inset to Figure 5. Probe rotation results in PS covering 13 orders of magnitude indicate that this is likely a very good approximation.[21]

We can use the expected behavior for the rotation and translation of a sphere in a hydrodynamic continuum in order to put these results into perspective. Using the Stokes–Einstein and Debye–Stokes–Einstein equations, one can calculate that the rms displacement for a sphere of radius $R$ in one rotational correlation time is $\sim 1.2R$ ($\sim$0.6 nm for tetracene) independent of temperature and viscosity. The results of this calculation are in reasonable agreement with what one calculates using the experimentally observed $D_T$ and $\tau_c$ for tetracene in *o*-terphenyl at high temperatures;[20] under these conditions, $\langle r^2 \rangle \approx 6D_T\tau_c = (0.4\ \text{nm})^2$. Thus, the results observed for tetracene in PS are remarkable in two respects: (1) translation is significantly enhanced over what is expected in a normal liquid, and (2) the relationship between translation and rotation changes significantly with temperature. The same pattern is observed for rubrene in PS, although here the deviations from the expected behavior are not as dramatic.

**Spatially Heterogeneous Dynamics.** Ehlich and Sillescu[4] previously reported that probe translation in PS has a weaker temperature dependence than $\eta$ (or $\eta/T$). They showed that a free volume treatment could account for their observations if it is assumed that probe motions are partially decoupled from those of the host. While the translational diffusion of rubrene and tetracene has a weaker temperature dependence than $\eta$, the rotational motion of these probes shows essentially the same temperature dependence as $\eta$. A straightforward application of the free volume approach would lead to the conclusion that translational motion is partially decoupled from matrix motions while rotational motion is fully coupled. In this section we present an alternate explanation which assumes that both the rotational and translational motion of the probes are fully coupled with matrix motions.

All of the observations presented here can be explained if the local dynamics of PS are spatially heterogeneous; i.e., some regions of the PS matrix have significantly faster local dynamics than neighboring regions (perhaps 5–10 nm away). The most direct evidence for this conclusion is Figure 7b. The nonexponential decay clearly indicates that $\langle r^2 \rangle/t$ has not reached its asymptotic limit on the length and time scales of this experiment. In other contexts, such anomalous diffusion has often been explained in terms of spatial heterogeneity. Examples include probe diffusion around filler particles in a composite[38] and solvent diffusion through polymer gels,[39] around glass beads,[40] and within spherical droplets.[41] The present case is different from the above examples in that our system has essentially only one component (PS).

Qualitatively, in a system where the local translational mobility is spatially heterogeneous, one expects to observe diffusive transport on time and length scales long enough that the diffusing species have fully sampled all possible environments. Since the effective length

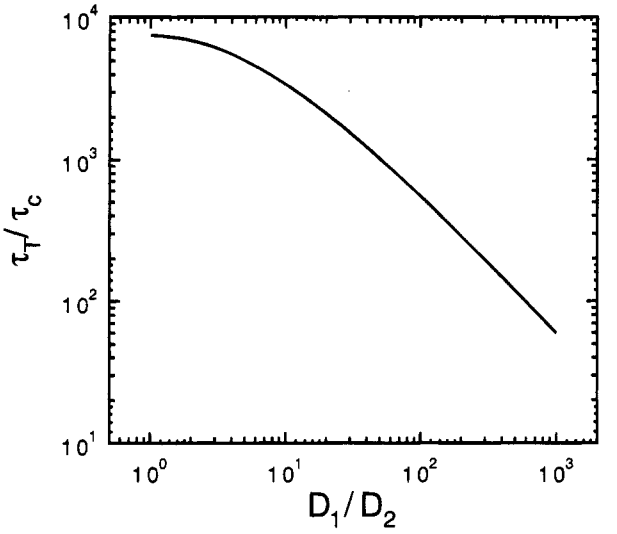


**Figure 8.** Model calculation illustrating that spatial heterogeneity can enhance translation relative to rotation by orders of magnitude. The system contains regions that are equally likely to have one of two local diffusion coefficients, $D_1$ and $D_2$. Calculation was performed using eq 12 of ref 45, with $p_1 = p_2 = 0.5$, $\tau = \infty$, $\langle r_2 \rangle = (60\ \text{nm})^2$, and a Stokes' radius $R = 0.6$ nm.

scale of the experiment in Figure 7 is roughly 60 nm (the rms displacement during $\tau_T$ assuming diffusive motion), we estimate that the heterogeneities responsible for the nonexponential decay in Figure 7b are not too much smaller than 60 nm, perhaps 10 nm. We know of no theory or simulation that would allow a quantitative estimate of this size based on our results.

Spatially heterogeneous dynamics also provide a natural explanation for the enhancement of translational motion relative to rotation (Figures 5 and 6), as recently discussed by Chang et al.,[42] Kivelson and Tarjus,[43] and Cicerone.[44] In a spatially heterogeneous system, the rotation and translation experiments average dynamics in very different ways. The rotation experiment is a snapshot which produces a weighted average of the rotational behavior in different regions; hence the observed rotation correlation function is nonexponential.[22] The correlation time $\tau_c$, defined as the integral of the correlation function, is heavily influenced by the slowest regions, since they cause the correlation function to have a long tail and a large integral. The translation experiment, on the other hand, measures the time required to traverse a fixed distance. $D_T$ is primarily influenced by the most mobile regions since distance is covered very quickly in these regions.

The different averaging of the rotation and translation experiments can be illustrated by a simple calculation. Zwanzig has used an effective medium approximation to calculate the effective diffusion coefficient $D_{eff}$ for a system that has two possible local diffusion coefficients, $D_1$ and $D_2$, which occur with a probability of $p_1$ and $p_2$.[45] Recent computer simulations have shown that the Zwanzig calculation is accurate.[46] For concreteness, we pick $p_1 = p_2 = 0.5$ and the lifetimes of the local regions to be infinite. By assuming that the Debye–Stokes–Einstein and Stokes–Einstein equations apply in each local region, we can calculate the local rotation times, $\tau_1$ and $\tau_2$, from $D_1$ and $D_2$. For this system, $\tau_c = 0.5(\tau_1 + \tau_2)$, while the time required to diffuse a distance $\langle r^2 \rangle$ is $\tau_T = \langle r^2 \rangle/(6D_{eff})$.

Figure 8 shows that translation becomes faster rela-

tive to rotation as the system becomes more heterogeneous. The effect of heterogeneity can be very large. We speculate that $D_T$ and $\tau_c$ have different temperature dependencies (Figure 5) because the segmental dynamics of PS become more heterogeneous as the temperature is lowered. This is consistent with probe rotation studies which indicate that the relaxation time distribution broadens as the temperature is lowered.[47] We speculate that the temperature dependencies of $D_T$ and $\tau_c$ for rubrene are more similar than for tetracene because the larger probe (rubrene) effectively averages over some of the matrix heterogeneity. This is consistent with the narrower distribution of rotational relaxation times observed for rubrene than for tetracene.[22] The lifetimes of the regions of different dynamics are also likely to play a role in a quantitative understanding of the different temperature dependencies of rotation and translation. Implicit in the above discussion is the assumption that the heterogeneities are long-lived compared to $\tau_T$.

What might be the origin of local variations in the translational mobility? Although our experiments provide no insight into this question, we suspect that local density variations (or free volume fluctuations) are responsible. According to Cohen and Turnbull,[48] $D_T$ is approximately proportional to $e^{-(1/f)}$, where $f$ is the free volume fraction. If we take $f(T_g) = 0.025$, then local fluctuations of ±6% in $f$ would produce more than a 100-fold variation in $D$. The corresponding density fluctuation would be only ±0.15%. A similar result can be obtained without using free volume theory.[49] Small length scale density fluctuations of this magnitude have been shown to exist in small molecule glass formers[50] and thus seem reasonable in PS. Density fluctuations whose magnitude varied only weakly with temperature would produce larger variations in $D_T$ at lower temperatures since dynamics become more sensitive to density (or free volume) fluctuations at low temperature. This could explain the increasing heterogeneity apparent in our experiments as the temperature is lowered.

Because spatially heterogeneous dynamics in PS likely occur over a broad range of time and length scales, the two-state model of Zwanzig is not a good candidate for quantitative calculations. The rotational correlation functions for rubrene and tetracene indicate a broad unimodal distribution of relaxation times.[22] The Zwanzig model also does not predict the length or time scales upon which translation becomes diffusive; such information is required for a quantitative interpretation of Figure 7b.

Our view that local dynamics in PS are spatially heterogeneous is supported by recent work on PS and other polymers.[51-54] Li et al. interpreted NMR spin diffusion experiments on polycarbonate as indicating distinct dynamic domains on the order of 3 nm in polycarbonate at $T_g$ + 50 K.[55] Several groups have reported that photochemical reactions in polymer matrices near $T_g$ do not follow first-order kinetics, with deviations becoming more significant at lower temperatures.[56-58] These results can be interpreted in terms of spatial variations in the local mobility of the polymer matrix.[56,57] Evidence also exists for spatially heterogeneous dynamics near $T_g$ in other glass-forming materials.[49,59]

**Anisotropic Diffusion?** As noted above, our results show that tetracene molecules in PS at 363.5 K translate an average of ~50 times their length in the average time required for a tetracene to rotate. Spatially heterogeneous dynamics can at least qualitatively explain this result. A different explanation postulates that each tetracene molecule translates extremely anisotropically. No spatial heterogeneity is required in this explanation.

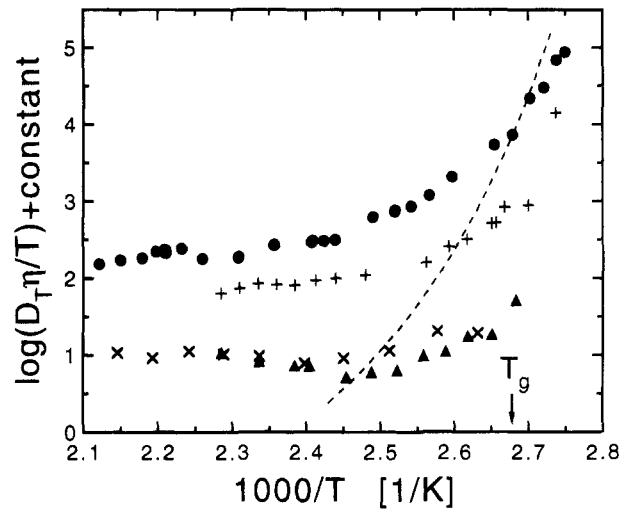


**Figure 9.** Comparison of the diffusion coefficients of various probes in PS: (●) tetracene; (+) 2,2′-bis(4,4-dimethylthiolan-3-one (TTI) (▲) rubrene; (×) cyclophane, tetraethyl[3.3](1,4)-naphthaleno-(9,10)anthracenophane-2,2,15,15 tetracarboxylate). The dashed line is a fit reported in ref 12 for diffusion of the photoproduct of thymoquinone. A flat line in this figure would indicate that $D_T$ has the same temperature dependence as $T/\eta$. $\eta(T)$ for 50 K PS was used in calculating the ordinate.

We have made no observation that rules out this explanation. However, we do not find this explanation plausible for four reasons: (1) Rubrene shows substantial rotational/translational decoupling and is shaped like a thick disk; anisotropic translation would seem improbable. (2) In a small molecule glass former, it has been shown that a more isotropic probe may exhibit translational motion which is decoupled from rotation to a greater extent than a more anisotropic probe.[19] (3) Although this model could produce anomalous diffusion, it would not produce a $c(t)$ decay on two time scales (such as Figure 7b). (4) The dimensions of tetracene are about 3.6 Å × 6.5 Å × 12.5 Å; this does not seem anisotropic enough to make this plausible. While one could imagine that holes open up and allow translation along the long axis, holes this large in other positions around the tetracene could well allow partial reorientation.

**Comparison to Other Work.** Ehlich and Sillescu[4] and Kim et al.[5] have measured translational diffusion of TTI and a cyclophane dye in PS, respectively. Their results are shown together with ours in Figure 9. The results are plotted as $D_T\eta/T$ in order to emphasize deviations from the temperature dependence predicted by eq 13. For the purposes of a rough comparison, we can consider tetracene and TTI to be of similar size (molecular weights of 228 and 256, respectively). Rubrene and the cyclophane dye are both considerably larger (molecular weights of 532 and 674, respectively).

Figure 9 indicates that the diffusion coefficients of rubrene and tetracene fit in reasonably well with diffusion coefficients reported in refs 4 and 5. Rubrene and cyclophane have smaller diffusion coefficients than TTI or tetracene, as expected. Diffusion of the larger probes track the temperature dependence of the viscosity more closely than the smaller probes. This last trend is consistent with the hypothesis that spatially hetero-

geneous dynamics are responsible for the enhanced translational diffusion observed at low temperatures.

Xia and Wang measured diffusion coefficients for a number of small probes in PS.[12] Their results for the photoproduct of thymoquinone are shown as a dashed line in Figure 9. Thymoquinone and its photoproduct are both smaller than tetracene. While the large values of $D_T$ at low temperatures are consistent with other results in the figure, the small values of $D_T$ at high temperatures are difficult to understand.

Although previous work has not compared the rotation and translation of a given probe in a polymer matrix, Ehlich and Sillescu[4] made an observation that is consistent with a key feature of our results. Reference 4 reported that a portion of the signal observed in their FRS experiments was independent of the grating spacing. Below $T_g$, the time scale of this decay was comparable to the time required for translation when the grating spacing was small. In retrospect, it seems likely that the unusual signal was due to probe rotation. Using this interpretation, their results are qualitatively consistent with our observations in figure 6.

## V. Concluding Remarks

We have shown that the translational diffusion coefficients of rigid probes in polystyrene can have a significantly weaker temperature dependence than the rotational correlation times of the same probes. For tetracene, this results in diffusion coefficients 4 orders of magnitude larger than would be expected on the basis of rotational correlation times and the assumption of a homogeneous matrix. The nondiffusive translational motion observed for tetracene at low temperatures suggests that the segmental dynamics of PS near $T_g$ are spatially heterogeneous on a length scale on the order of 10 nm.

Spatial heterogeneity can qualitatively account for the different temperature dependences observed for probe rotation and translation in polystyrene. Probe rotation times are dominated by the dynamics of slowly relaxing regions while translational diffusion coefficients are heavily influenced by the more mobile regions. If heterogeneity is responsible for enhancing translational diffusion near $T_g$ by orders of magnitude, then the use of free volume theory to interpret results like these must be reassessed. The versions of free volume theory used to interpret probe translational diffusion coefficients generally assume a spatially homogeneous system.

Based on our observations and those of other investigators, spatially heterogeneous dynamics appear to be an important feature of many bulk amorphous polymers near $T_g$. The combination of probe rotation and translation experiments is quite sensitive to spatial heterogeneities and could be used to compare heterogeneity in different polymers. Given the appropriate theories or simulations, such observations could be used to characterize the length scale of heterogeneities and the extent to which dynamics vary from region to region.

**Acknowledgment.** We thank George Maret and Bob Hamers for their helpful suggestions regarding the holographic FRAP apparatus, and John Ferry, Dan Kivelson, Roger Loring, Jim Skinner, Frank Stillinger, Ernst von Meerwall, and Hyuk Yu for useful discussions. Acknowledgment is made to the National Science Foundation (DMR-9424472) and the donors of The Petroleum Research Fund, administered by the American Chemical Society, for support of this research.

## References and Notes

(1) See, for example: Fujita, H. *Adv. Polym. Sci.* **1961**, *3*, 1.
(2) Korsmeyer, R. W.; von Meerwall, E. D.; Peppas, N. A. *J. Polym. Sci., Polym. Phys. Ed.* **1986**, *24*, 409.
(3) Waggoner, R. A.; Blum, F. D. *J. Coat. Technol.* **1989**, *61* (768), 51.
(4) Ehlich, D.; Sillescu, H. *Macromolecules* **1990**, *23*, 1600.
(5) Kim, H.; Waldow, D. A.; Han, C. C.; Tran-Cong, Q.; Yamamoto, M. *Polym. Commun.* **1991**, *32*, 108.
(6) von Meerwall, E. D.; Ferguson, R. D. *J. Appl. Polym. Sci* **1979**, *23*, 3657.
(7) Moore, R. S.; Ferry, J. D. *J. Phys. Chem.* **1962**, *66*, 2699. Wong, C. P.; Schrag, J. L.; Ferry, J. D. *J. Polym. Sci., A-2* **1970**, *8*, 991.
(8) Chen, S. P.; Ferry, J. D. *Macromolecules* **1968**, *1*, 270. Probe translational diffusion data in natural rubber should be compared with the viscosity data in: Gotro, J. T.; Graessley, W. W. *Macromolecules* **1984**, *17*, 2767.
(9) Arnould, D.; Laurence, R. L. *Ind. Eng. Chem. Res.* **1992**, *31*, 218.
(10) Landry, M. R.; Gu, Q. J.; Yu, H. *Macromolecules* **1988**, *21*, 1158.
(11) Frick, T. S.; Huang, W. J.; Tirrell, M.; Lodge, T. P. *J. Polym. Sci., Polym. Phys. Ed.* **1990**, *28*, 2629.
(12) Xia, J.; Wang, C. H. *J. Polym. Sci., Polym. Phys. Ed.* **1995**, *33*, 899.
(13) Mears, P. *J. Am. Chem. Soc.* **1954**, *76*, 3415.
(14) Berens, A. R.; Hopfenberg, H. B. *J. Membr. Sci.* **1982**, *10*, 283.
(15) Gusev, A. A.; Suter, U. W. *J. Chem. Phys.* **1993**, *99*, 2228.
(16) Masuko, T.; Sato, M.; Karasawa, M. *J. Appl. Polym. Sci.* **1978**, *22*, 1431.
(17) Vrentas, J. S.; Duda, J. L.; Ling, H.-C. *J. Polym. Sci., Polym. Phys. Ed.* **1985**, *23*, 275.
(18) Fujara, F.; Geil, B.; Sillescu, H.; Fleischer, G. *Z. Phys. B* **1992**, *88*, 195.
(19) Cicerone, M. T.; Ediger, M. D. *J. Chem. Phys.*, to be submitted.
(20) Rossler, E.; Eiermann, P. *J. Chem. Phys.* **1994**, *100*, 5237.
(21) Blackburn, F. R.; Cicerone M. T.; Ediger, M. D. *J. Polym. Sci. B: Polym. Phys.* **1994**, *32*, 2595.
(22) Inoue, T.; Cicerone, M. T.; Ediger, M. D. *Macromolecules* **1995**, 28, 3425.
(23) We observed no change in dynamics in the samples with time, even after cycling through temperatures up to 410 K several times, and after the samples had been left in silicone oil for many months.
(24) Davoust, J.; Devaux, P. F.; Leger, L. *EMBO J.* **1982**, *1*, 1233.
(25) These expressions assume equal intensity beams. Unequal beam intensities lower the signal-to-noise ratio but do not change the shape of $c(t)$ (see eq 8). Throughout this section we ignore the spatial profile of the laser beams. Reference 26 has treated the case when the spot sizes become comparable to d.
(26) Imhof, A.; van Blaaderen, A.; Maret, G.; Mellema, J.; Dhont, J. K. G. *J. Chem. Phys.* **1994**, *100*, 2170.
(27) Eichler, H. J.; Gunter, P.; Pohl, D. W. *Laser-Induced Dynamic Gratings*; Springer: Berlin, 1986.
(28) Cicerone, M. T.; Ediger, M. D. *J. Phys. Chem.* **1993**, *97*, 10489.
(29) van Blaaderen, A.; Peetermans, J.; Maret, G.; Dont, J. K. G. *J. Chem. Phys.* **1992**, *96*, 4591.
(30) Smith, B. A.; Samulski, E. T.; Yu, L. P.; Winnik, M. A. *Phys. Rev. Lett.* **1984**, *52*, 45. These authors used no modulation. Vibrations during reading would make this approach difficult for small grating periods.
(31) This statement is true for permanent photobleaching. If the photobleach is at least partially reversible, the translational motion of the transiently bleached species is also detected to some extent. In these experiments, partially reversible photobleaching was observed for both probes at the highest temperatures. The extent of reversible photobleaching was negligible except above 450 K for tetracene. Even under these conditions, the potential error in the log $D$ due to this effect is less than 0.1.
(32) Wegener, W. A.; Rigler, R. *Biophys. J.* **1984**, 46, 787. Wegener, W. A. *Biophys J.* **1984**, *46*, 795.
(33) Smith, B. A.; McConnell, H. M. *Proc. Natl. Acad. Sci. U.S.A.* **1978**, *75*, 2759.
(34) Lanni, F.; Ware, B. R. *Biophys. J.* **1984**, *46*, 97.

(35) Mustafa, M. B.; Tipton, D. L.; Barkley, M. D.; Russo, P. S.; Blum, F. D. *Macromolecules* **1993**, *26*, 370.
(36) Park, S.; Yu, H.; Chang, T. *Macromolecules* **1993**, *26*, 3086.
(37) As described in ref 21, polystyrene viscosity data were taken from: Plazek, D. J. *J. Phys. Chem.* **1965**, *69*, 3480. Schausberger, A.; Schindlauer, G.; Janeschitz-Kriegl, H. *Rheol. Acta* **1985**, *24*, 220.
(38) von Meerwall, E. D. *Rubber Chem. Technol.* **1985**, *58*, 527.
(39) Ilyina, E.; Daragan, V. *Macromolecules* **1994**, *27*, 3759.
(40) Callaghan, P. T.; Coy, A.; MacGowan, D.; Packer, K. J.; Zelaya, F. O. *Nature* **1991**, *351*, 467.
(41) Tanner, J. E.; Stejskal, E. O. *J. Chem. Phys.* **1968**, *49*, 1768.
(42) Chang, I.; Fujara, F.; Geil, B.; Heuberger, G.; Mangel, T.; Sillescu, H. *J. Non-Cryst. Solids* **1994**, *172–174*, 248.
(43) Tarjus, G.; Kivelson, D. *J. Chem. Phys.* **1995**, *103*, 3071.
(44) Cicerone, M. T. Ph.D. Thesis, University of Wisconsin, Madison, WI, 1994.
(45) Zwanzig, R. *Chem. Phys. Lett.* **1989**, *639*, 164.
(46) Cicerone, M. T.; Ediger, M. D., unpublished results.
(47) For example, the KWW $\beta$ parameter for BPEA rotation in PS changes from 0.65[21] at high temperature to 0.50[44] at $T_g$.
(48) Cohen, M. H.; Turnbull, D. *J. Chem. Phys.* **1959**, *31*, 1164.
(49) Cicerone, M. T.; Ediger, M. D. *J. Chem. Phys.* **1995**, *103*, 5684.
(50) Fischer, E. W. *Physica A* **1993**, *201*, 183.
(51) Spiess and co-workers used multidimensional NMR experiments to measure the dynamics of subensembles of relaxing elements in poly(vinyl acetate) and polystyrene.[52,53] While these results were originally interpreted as indicating long-lived spatial heterogeneity, they have recently been reinterpreted.[54]
(52) Schmidt-Rohr, K.; Spiess, H. *Phys. Rev. Lett.* **1991**, *66*, 3020.
(53) Leisen, J.; Schmidt-Rohr K.; Spiess, H. W. *Physica A* **1994**, *201*, 79.
(54) Heuer, A.; Wilhelm, M.; Zimmermann, H.; Spiess, H. W. *Phys. Rev. Lett.*, submitted.
(55) Li, K.-L.; Jones, A. A.; Inglefield P. T.; English, A. D. *Macromolecules* **1989**, 22, 4198.
(56) Richert, R. *Macromolecules* **1988**, *21*, 923.
(57) Eisenbach, C. D. *Ber. Bunsenges. Phys. Chem.* **1980**, *84*, 680.
(58) Victor, J. G.; Torkelson, J. M. *Macromolecules* **1987**, *20*, 2241.
(59) Moynihan, C. T.; Schroeder, J. *J. Non-Cryst. Solids* **1993**, *160*, 52.

MA951033F